Article:
Kunchimon, SZ, Tausif, M, Goswami, P et al. (2020) From hybrid fibers to microfibers: The characteristics of polyamide 6/polypropylene blend via one-step twin-screw melt extrusion. Polymer Engineering and Science, 60 (4). pp. 690-699. ISSN: 0032-3888

https://doi.org/10.1002/pen.25327

Title

From hybrid fibres to microfibres: the characteristic of polyamide 6/polypropylene blend via one-step twin-screw melt extrusion

Running title

Polyamide 6/polypropylene hybrid fibres to microfibres

Authors

Siti Zaharah Kunchimon [1,2], Muhammad Tausif [2], Parikshit Goswami [3] and Vien Cheung [2]

[1] Department of Mechanical Engineering, Faculty of Engineering Technology, Universiti Tun Hussein Onn Malaysia, 86400, Batu Pahat, Johor, Malaysia

[2] School of Design, University of Leeds, Leeds, LS2 9JT, UK

[3] Technical Textiles Research Centre, School of Applied Science, University of Huddersfield, Huddersfield, HD1 3DH, UK

Correspondence: Siti Zaharah (email: zahara@uthm.edu.my)

Acknowledgements

The authors acknowledge the financial support from the Ministry of Education (MoE) of Malaysia and Universiti Tun Hussein Onn Malaysia (UTHM) for doctorate scholarship.

Abstract

Multi-material textiles are frequently employed to attain a certain function or aesthetic effect. The multi-material assemblies face recycling limitations due to challenges to sort and separate the component materials. A one-step melt extrusion approach to process two mixed common textile polymers, polyamide 6 (PA6) and polypropylene (PP), into PA6:PP hybrid fibres is reported in this study. PA6:PP hybrid fibres were produced in four different configurations; PA6-50 (50 wt% PA6), PA6-60 (60 wt% PA6), PA6-65 (65 wt% PA6) and PA6-80 (80 wt% PA6). The PP component was sacrificially removed from the hybrid fibres and the resultant PA6 fibre structure was analysed. The SEM images show the development of PA6 microfibres in PA6-50 and PA6-60 hybrid fibres with mean diameters of 0.76 µm and 1.13 µm upon fibre drawing, respectively. In PA6-65 hybrid fibres, the PA6 microfibres were found along with areas where PA6 was encapsulating the PP. Thermal and mechanical properties of the untreated and treated hybrid fibres were also investigated. PA6-60 hybrid fibres were processed into single jersey knitted fabrics and treated to obtain PA6 microfibres fabrics. The bursting strength and wicking properties of the fabric, before and after treatment, were comparatively studied.

Keywords: Polyamide, microfibres, thermoplastics, blends, melt spinning, recycling

Introduction

Recycling

Demand in textiles consumption are predicted to increase more than three times by 2050 which will invariably increase the use of non-renewable material sources needed in textile production.[1,2] Huge amount of textiles products already end up in landfill or being incinerated at the end of their useful life. Over two-third of textile raw materials use non-renewable resources and the main non-renewable polymers include polyamide 6 (PA6) and polypropylene (PP). In carpet industry, PP is used as a carpet backing and PA6 is used as the face fibre on the carpet surface. PA6 and PP are thermoplastic polymers and can be recycled several times, however, mix-materials consist in textile products limit the recycling potential unless specific recycling strategies could be adopted. Melt-extrusion applies thermo-mechanical processes can be used to recycle mixed-waste thermoplastic polymers such as PA6 and PP.

Fibre morphology

Blending of two immiscible polymers such as PA6 and PP produces several morphologies depending on the production processes involved. The chemical interaction between these polymers are low[1,3] and therefore the blending of these polymers produces poor surface interfacial adhesion. Mixing or extrusion of PA6:PP blend in compressed moulding and injection moulding under appropriate procession conditions produce droplet-matrix morphology[4–6] while fibril-matrix morphology occurred with the presence of elongation force during melt extrusion or drawing process.[7–10] Several studies show the development of "island-in-the-sea effect" of the extruded fibre produced by blending PA6 and PP with the help of compatibiliser.[7,8,11] The compatibiliser improves the surface adhesion between the polymers and create the PA6 fibrils which are hardly formed without compatibiliser.

The blend composition of the component polymers has an effect on the morphology of the resultant fibres. Our previous study shows that the blending of two partially miscible polymers; PA6 and thermoplastic polyurethane produced interconnected multi-porous hybrid fibres structures.[12] Limited literature in this subject area reports that PA6 forms the disperse phase and PP forms the matrix phase in fibres where the PA6 component is less than 50 wt% of the hybrid fibres.[5,7–9] With PA6 as the minority polymer in the blend, the potential of PA6 to disperse in the PP matrix is high and the elongation force during extrusion helps to create the PA6 fibril (island) in the PP matrix (sea). Increasing PA6 in the blend increases the number of droplets/fibrils and produce coarser morphology of the PA6 droplet or fibril.[5,11,13] PA6 starts behaving like a matrix phase when the wt% of PA6 is more than 60.[9,14]

Objectives

In this study, one step blending/melting was used to produce monofilament PA6:PP hybrid fibres. The objectives of this work are to investigate i) the effect of blending PA6 and PP with PA6 composition dominant in the fibre (50-80%), ii) the potential of producing PA6:PP hybrid fibres via one-step twin-screw melt extrusion with the absent of compatibiliser, iii) the morphology, mechanical and thermal properties of PA6:PP hybrid fibres before and after removing PP component from the fibres, iv) the potential to produce knitted fabric using monofilament PA6:PP hybrid fibres. This work investigates the effect of blending mix-waste materials consist of PA6 and PP polymers extruded into hybrid fibres with PA6 component dominant in the blend. The blending of two immiscible polymers are expected to produce matrix-fibril fibre morphology with the presence of elongation force after the extrusion process.

Experimental

Materials

The polyamide 6 (PA6) pellets (*Radilon S 35F 100NT*) were purchased from Radici Group, Gandino, Italy and the polypropylene (PP) pellets (Capilene® T 89 E) were purchased from Carmel Olefins Ltd, Israel. The PA6 pellets were dried in an oven at 100°C for at least 6 h before manually mixing with PP pellets. Different PA6:PP blend compositions were prepared at the weight ratios of 100:0 (PA6), 80:20 (PA6-80), 65:35 (PA6-65), 60:40 (PA6-60), 50:50 (PA6-50), and 0:100 (PP).

Methods

Fibre production

A 10 mm twin-screw extruder (Rondol Technology Ltd., UK; *Rondol-Microlab*; screw dimension (L/D) 20:1; die diameter 2 mm) was used to extrude PA6:PP hybrid fibres (as-spun untreated hybrid fibres). The temperature profile of the twin-screw extruder from feed hopper (zone 1), zone 2, zone 3, zone 4 and die zone were set at 170, 200, 230, 230 and 230°C, respectively. The screw speed, take-up winder speed and the distance between the die and the winder were set at 60 rpm, 24.5 m min^{-1} and 1 m, respectively. Drawing process was done on tensile strength tester by stretching the fibre 250% from its original length (drawn untreated hybrid fibres). The as-spun and drawn hybrid fibres were treated with boiling toluene at 110 °C for 3 h to remove the PP component (as-spun treated and drawn treated fibres). Prior to testing, the fibres were conditioned at 20±2°C and a relative humidity of 65±5% for 24 h.

Morphology of fibres

The fibres morphology was examined using scanning electron microscopy (SEM) (Hitachi S-2600N). A gold coating was applied on the fibres in an Emitech K550X sputter coater and observed at 3 to 5 kV. The fibres were also cross-sectioned following AATCC Test Method 202159 and viewed under a light microscope (Leica M205C). The knitted fabrics were examined on SEM (Jeol JSM-6610LV) with 1000x magnification observed at 8 kV. The morphology of the hybrid fibres were predicted using Eq. 1, where η_i and ϕ_i represent the viscosity and volume fraction of the polymer *i* and where η_e and ϕ_e represent the viscosity and volume fraction of the polymer e. If the value obtain is ≤ 1, polymer *i* become a matrix, if the value is close to 1, phase inversion occurred and if the value is ≥ 1, polymer *e* becomes a matrix [15,16].

$$\frac{\eta_i}{\eta_e}\frac{\phi_e}{\phi_i} = 1 \qquad \text{Eq. 1}$$

Thermal properties

Thermal transition of the fibres (5-7 mg, cut from fibres, undried) were measured using differential scanning calorimetry (DSC) (TA Instruments; Q2000) with heating rate of 10 °C min^{-1} in the temperature range of 0 °C-250 °C (heat-cool-heat, Nitrogen (N_2): 25 mL min^{-1}). Melting temperature (T_m), crystallisation temperature (T_c) and melting enthalpy (ΔH_x) for both polymers were recorded. The percentage crystallinity of PA6 and PP was calculated using Eq. 2,[17] where ΔH_x is melting enthalpy of the polymer x, w_x is the weight percentage of polymer in the hybrid fibres and ΔH_x^0 is the value of melting enthalpy of completely crystalline polymer. ΔH_{PA6}^0 and ΔH_{PP}^0 are 230.1 J g^{-1} and 209.2 J g^{-1}, respectively, taken from literature.[17,18]

$$\%\, Crystallinity\ of\ X_x = \frac{\Delta H_x}{\Delta H_x^0 * w_x} \times 100 \qquad \text{Eq. 2}$$

Thermal degradation of the fibres (cut from fibres, undried) was carried out on a Thermogravimetric Analyzer (TGA) (TGA Q50) in the temperature range of 25 °C to 600 °C under nitrogen atmosphere (25 mL min^{-1}) at the heating rate of 10 °C min^{-1}.

Rheology properties

The apparent viscosity of the PA6 and PP was studied using capillary rheometry (Bohlin, RH2000; 16 mm barrel; 1 mm die diameter). The barrel temperature was set at 230 °C for all heating zones. 30 g polymer was filled in the barrel and then extruded through the die with the piston speed ranged between 1-30 mm min^{-1}. The viscosity ratio of both polymer blend was determined by Eq. 3.

$$Viscosity\ ratio, k = \frac{viscosity\ dispersed, \eta_d}{viscosity\ matrix, \eta_m} \qquad \text{Eq. 3}$$

Mechanical properties

The mechanical properties of single fibre were measured using tensile tester (Titan) (gauge length: 20 mm at 1000 mm min^{-1} crosshead speed). The average value of tensile strength (cN tex^{-1}) and elongation (%) were measured from at least 10 specimens. The diameter of the fibres was measured from SEM images using ImageJ software.

Fabric production

PA6-60 hybrid fibres were drawn on a draw frame machine with draw ratio of 2 before produced as single jersey knitted fabrics on a 10-gauge double-bed flat knitting machine. Subsequently, the fabrics were treated in boiling toluene for 3 h to remove the PP component. The fabric mass per unit area, thickness, number of courses and wales per inch and stitch density were measured from at least 3 samples from each fabric.

Wicking properties

The vertical wicking behaviour in course and wales direction was measured. Both untreated and treated fabric were dyed to quantify the wicking of water. Owing to different morphology of the fibres, untreated and treated fabrics were dyed using different approaches. The treated fabrics, where outer component was dominant by PA6, were immersed in the dye solution (0.15 g dm^{-3} Azonine Scarlet dye dissolved in 1 litre water) for 30 mins to get coloured fabric. The untreated fabrics, where the dominant component was PP, were dyed with Disperse Red 60 in lab-scale dyeing machine (Roaches Pyrotec 200) at 100 °C for 3 h. 2% of dye on the weight of the fabric was added with dispersing agent (Ufoxane 1%) and water to get a liquid to fabric ratio of 40:1. Acetic acid was used to adjust the pH of the dye to 4-4.5. The fabrics were washed in a soaping agent (2g/l Anionic detergent) for 15 mins at 70°C, rinsed and dried. The dyeing of PP-blended fibre was aided by the PA6 component acting as an amine modifier.[4] The dyed fabrics were cut in a rectangular specimen (9 cm x 2.5 cm). The specimen was suspended vertically with the bottom part immersed in the distilled water. The height of the water displacement by the fabric was recorded after 5, 10, 15 and 30 minutes.

Fabric strength

The strength of the fabrics was measured using Titan ball burst strength tester. The average value of fabric strength (N) were measured from at least of 3 specimens and normalised to the fabric mass (fabric strength (N)/fabric mass per unit area (g m^{-2})). Prior to testing, the fibres and fabric were conditioned at 20±2°C and a relative humidity of 65±5% for at least 24 h.

Results and discussions

Rheology

The morphology of the polymer blend is influenced by the viscosity of the blend. The viscosity of the PA6 and PP during melt extrusion can be obtained from the rheology curve of each polymer processed at 230 °C (see Figure S1 in Supporting Information). The shear rate during melt extrusion is 314 s^{-1}, calculated using Eq. 4[19] where the screw speed (*n*) is 60 rpm, screw outer diameter (*D*) is 10 mm and overflight gap (*h*) is 0.1 mm. From the calculation, the viscosity of both polymers at 314 s^{-1} shear rate is 1000 Pa.s and 150 s^{-1} for PA6 and PP, respectively.

$$Shear\ rate = \frac{\pi * D * n}{h * 60} \qquad \text{Eq. 4}$$

The morphology of the blend can be predicted using Jordhamo model as shown in Eq. 1. Based on the Jordhomo model, values obtained for the blends are shown in Table 1. PP was expected to become a matrix in all the blends due to its low viscosity. However, only PA6-60 and PA6-50 shows the expected morphology amongst all the hybrid combinations used in this study. PA6-80, due to the high weight ratio of PA6 in the blend, do not show the expected trend. Details of the fibres' morphology was discussed in the *Morphology of the fibres* section.

Morphology of the fibres

Types of polymer, blend composition and viscosity ratio are factors that contribute to the morphology of the hybrid fibres. PA6 and PP are immiscible and incompatible when blended and creates high interfacial tension resulting in distinct phase separation. Major component in the blend might forms the continuous matrix, and the minor component disperses in the matrix (see Figure S2 in Supporting Information) in the shape of droplets, spheres or fibrils depending on the production method (extrusion, compression or injection mould) and several other factors.

As mentioned above, the phase separation between PA6 and PP was expected. The structure of the PA6:PP fibre blends obtained in this study were grouped in two fibre structures; structure I and structure II, as shown in Figure 1 and Figure 2. PA6-50 and PA6-60 represents structure I where the morphology of the hybrid fibre shows a fibril-matrix structure with PP as the matrix and PA6 as the dispersed phase. Removing the PP component from these hybrid fibres results in obtaining PA6 microfibres (Figure 2 A-2 & B-2). Structure II (PA6-65 and PA6-80) presents the hybrid fibres with PA6 as a matrix and PP as a dispersed phase. When PA6 content in the fibres was increased to 65%, the phase inversion between PA6 and PP took place, but not completely inverted. The SEM images of the PA6-65 after treatment (Figure 2 C-2) show that the PA6 dominantly act as a matrix and dispersed as fibrils in certain areas. For PA6-80, the morphology of the fibre after treatment (Figure 2 D-2) does not show any changes, demonstrating that the PA6 component surrounds the dispersed PP completely.

Previous studies reported that the PA6 composition ranging from 6 to 50 weight percentage exhibit the development of PA6 as a dispersed phase and PP as a matrix.[5,7–9] Co-continuous structure or phase inversion between polymers normally happen when the weight ratio is almost the same[5,11] and PA6 start becoming a matrix when its content is 50% and higher.[14] In this study, PA6 was selected as a major component and the weight percentage were set at 50 to 80% in the blend. From the results obtained, PA6 was found dispersed in the PP matrix even when the composition of PA6 is higher in the blend. This could be due to the viscosity ratio of the blend.

The position of the polymer in the blend, based on Eq. 3, is dependent on the viscosity ratio of the blends. For PA6-80, PA6 is matrix and PP is dispersed phase, giving a viscosity ratio of 0.15. For PA6-60 and PA6-50, the viscosity ratio of both blends is 6.7 when considering PP as a matrix phase. High viscosity ratio can lead to bigger droplet/fibril dispersed in the matrix while low viscosity ratio contributes to the better dispersion of the blend.[20]

The viscosity ratio of the blends when PP become a matrix phase is high in this study due to the high viscosity of PA6. The low viscosity of PP in the blend makes it flow easily and thus PP encapsulates the high viscous PA6 when the blend ratio is almost the same (PA6-50 and PA6-60). For PA6-65, phase inversion happens and the PA6 start to take over matrix position even though the PP has low viscosity. In PA6-80, PA6 completely become the matrix phase. The PA6 was dried upon processing in order to remove the moisture in the polymer. PA6 is a hygroscopic polymer which has potential to absorb moisture from the environment.[21] The presence of moisture during processing can cause hydrolysis, a chemical reaction that break the polymer chain and reduce the polymer viscosity, decrease mechanical strength and other properties.[22] The morphology of the hybrid fibres might changes with the presence of moisture, however, further investigation can be done to study this phenomenon.

The diameter of the as-spun fibres exhibits no specific trend in term of the amount of PA6 content in the hybrid fibres as shown in Figure 3 (see Figure S3 in Supporting Information for diameter trend). Among the hybrid fibres, PA6-60 displays the largest fibre diameter with mean value of 174±8.1 µm while PA6-65 has the smallest diameter with 105±16.7 µm.

The average diameter of PA6 microfibres for PA6-50, PA6-60 and PA6-65, obtained from treated as-spun fibres, are 1.95, 1.74 and 1.36 µm, respectively, shown in Figure 4. The diameter of PA6 microfibres obtained using single step twin-screw melt extruder presented almost similar diameter of fibres obtained from electrospinning[23] and carbon dioxide laser supersonic drawing.[24] The diameter of as-spun PA6 microfibres decreased when the PA6 content was increased. Other studies reported that the increasing of PA6 content in the blend results in coarser morphology of the PA6 droplet or fibril.[5,11,13] The hybrid fibres were then stretched to 250% of its original length and treated in toluene to obtain drawn PA6 microfibres. The diameter of drawn PA6 microfibres decreases 30-60% after stretching; PA6-50 has the lowest fibril diameter (Figure 4). The diameter of the microfibres are well distributed after drawing (see Figure S4 in Supporting Information).

The PA6 microfibres were obtained after the removal of PP component using organic solvent toluene. Long exposure to toluene can have adverse effects on human health and therefore,[25] in future work, other solvents such as appropriate water-free green-solvents (e.g. ionic liquids) could be used. Moreover, the PP dissolved in the toluene can be used again to produce PP micro/nanofibres using electrospinning method.[26] Recycling of solvents in fibre production is well known and is used commercially by fibre producers.[27]

Thermal properties

The melting temperature of PA6 and PP were 221 °C and 160 °C, respectively, measured using DSC (Figure 5 Untreated). For as-spun hybrid fibres, two clear endothermic peaks for PA6 and PP were observed in the second heating cycle as shown in Figure 5 (untreated), demonstrating the immiscibility of the blend. Maximum melting temperature (T_m) of PA6 remain unaffected in all hybrid fibres which completely melted at 221 °C, same as PA6 fibre (Table 2). A shoulder peak appears at around 215 °C in pure PA6 and all hybrid fibres, close to PA6 melting temperature, indicating the alteration of PA6 crystal morphology after the first heating cycle.[28,29]

The same trend was observed in the cooling cycle of as-spun fibres with two exothermic peaks of PA6 and PP separated (see Figure S5 in Supporting Information). The crystallisation temperature (T_c) of as-spun PA6 hybrid fibres are almost the same as pure PA6. For PP, the exothermic peak shifts to higher temperature and this corresponds to the increment of PA6 content in the blend. During the cooling process, the PA6 which solidifies at a higher temperature (~188 °C) crystallise without difficulty as the PP is still in the molten state. Therefore the crystallisation temperature of PA6 was not particularly affected. The solidified PA6 in the blend then, however, enhance the nucleation rate of PP, thus affect the PP crystallisation temperature.[3,30]

The percentage of crystallinity for PA6 and PP in the as-spun untreated hybrid fibres are lower than single fibres component (Table 2). The decrease of the crystallinity could be attributed to the ability of the polymers to form crystal domain. During blending of immiscible polymers, the barrier could have been developed from the second component disturbing the crystal formation[26] and the results correspond to the study by Jaziri.[3]

The as-spun fibres were treated with toluene to remove the PP component in the hybrid fibres, and the thermal properties of the treated fibres are shown in Figure 5 (Treated) and Table 3 (see also Figure S5 in Supporting Information). After the treatment, two different PA6 structures were identified as mentioned in *Morphology of fibres* section.

In Structure I, PA6-50 and PA6-60, the PP component was completely removed from the hybrid fibres, with no obvious peaks observed. In Structure II, PA6-80 and PA6-65 hybrid fibres, PA6 was found to be in a matrix phase and encapsulated most of the PP component inside the matrix. The DSC curves confirm that the PP component remains in the Structure II after the treatment. No significant changes of melting and crystallisation temperature of both components were observed for the treated fibres (Table 3). The melting enthalpy of PA6-80 slightly decreased in both PA6 and PP components after the treatment. In PA6-65, the melting enthalpy of PP decreased while for PA6 it increased. The removal of small amount of PP in PA6-65 influenced the melting enthalpy of both polymers.

Figure 6 shows the TGA curve and derivative weight curve of the as-spun hybrid fibres (untreated). The thermal decompositions of as-spun hybrid fibres are in between that of the parent polymers except for PA6-65 (Table 4). The exceptional behaviour of PA6-65 can be seen clearly in derivative weight curve with a small shoulder peak at 466 °C (thermal decomposition temperature at 434 °C). The partially co-continuous morphology of the PA6-65 fibres might influence the thermal decomposition of the fibres. PP fibres has higher decomposition temperature at 460 °C and PA6 decomposes at 450 °C.

For treated fibres, the Structure I (PA6-60 and PA6-50 hybrid fibres) shows reduction in decompose temperature compared to the fibres before treatment (see Figure S6 in Supporting Information). PA6 microfibres were existed in this structure, thus displaying similar decomposition behaviour with PA6 fibres. In treated PA6-65, similar trend can be observed with untreated fibres showing small shoulder peak after the maximum decomposition temperature. The morphology of these hybrid fibres after treatment, having the PA6 as matrix and PP as microfibres, give rise to this behaviour.[31]

Mechanical properties

Figure 7 shows the tenacity of the as-spun and drawn fibres (both treated and untreated). The tenacity of the as-spun hybrid fibres is almost similar or slightly lower than PA6, and higher than that of PP fibres. The strength of the fibres is related to the morphology of the fibres. In Structure I, the as-spun PA6-65 (untreated) exhibits higher strength than other hybrid fibres while PA6-80 has the lowest strength. In Structure II (PA6-50 and PA6-60), the strength of the hybrid fibres was slightly higher than PA6-80 and lower than PA6-65. The function of the polymers, either matrix or dispersed, contribute to the strength of the hybrid fibres. The PA6 solidifies quicker than PP as demonstrated by DSC curves (see Figure S5 in Supporting Information). Therefore, when PA6 is outside, the PP inside is yet to solidify resulting in shrinkage and gaps between PA6 and PP interfacial surface.[32] On contrary, when PA6 is the inner component, PP can solidify on PA6 resulting in better interfacial adhesion of the blend. Good adhesion between PA6 and PP when PA6 is inside (Structure I) contribute to the improved strength of the PA6-60 and PA6-50 hybrid fibres. The same trend can be seen for untreated drawn fibres, where Structure I have slightly higher tenacity than Structure II. Untreated as-spun PA6-65, displays higher strength than other hybrid fibres; this could be attributed to the unique structure (Figure 1) of PA6 and PP in the fibres.

For drawn hybrid fibres, the strength of the hybrid fibres shows 114-230% improvement compared to the as-spun fibres. The increase is due to the better orientation and crystallinity of the fibres during the drawing process.[33]

After the treatment with toluene, the tenacity of the as-spun treated PA6-80 fibres slightly increased while for the other as-spun treated hybrid fibres, the strength decreased. The removal of the PP component in the hybrid fibres lead to the decrease of the fibre strength. PA6 is the dominant component in PA6-80 fibres and it also acts as the matrix, thus PA6-80 was not affected by the treatment as much as other fibres. PA6-65 after treatment developed cracks in the hybrid fibres (Figure 2 C-2, C-3 & C-4). This structural change contributed to the decrease in the fibre strength of PA6-65. In PA6-60 and PA6-50 only PA6 microfibres were left after the treatment (Figure 2 A-2 & B-2) and therefore resulted in the reduction of the fibre strength. For drawn fibres, the strength of the hybrid fibres after treatment also decreased except for PA6-60.

As-spun and drawn hybrid fibres (untreated) show that the Structure I have lower breaking elongation compared to Structure II (see Figure S7 in Supporting Information). Structure I have good adhesion between the polymer surfaces (compared to Structure II) and this restricts the movement of the polymers, thus has lower breaking elongation than Structure II. After the removal of PP component, the breaking elongation of the treated hybrid fibres (as-spun and drawn) were observed to decrease. This can be attributed to aligned polymer chains in fibrous form compared to higher extension of fibres with both fibre and matrix components.

Figure 8 shows the representative curves of tenacity versus elongation for the drawn (untreated and treated) hybrid fibres (see Figure S8 in Supporting Information for as-spun hybrid fibre). The curves of the untreated PA6-60 and PA6-50 hybrid fibres (as-spun and drawn) show two breaking points (shown with pointed arrows in Figure 8). Both hybrid fibres have PP as the matrix and PA6 as the microfibers. These microfibers influence the breaking elongation of the fibres. The first breaking point happens when the PP matrix and PA6 microfibres that are close to the fibre surface fail and break. The second breaking point is due to the failure of the PA6 microfibres located at the centre of the fibres. The second breaking point could also be seen on PA6-60 treated fibres.

The Young's modulus of the as-spun and drawn hybrid fibres (untreated) were higher than PA6 but almost the same with PP fibres except for PA6-80 as-spun fibres (see Figure S9 in Supporting Information). The Young's modulus for as-spun treated and untreated fibres are very similar. Drawn treated hybrid fibres for Structure I displays high Young's modulus compared to the untreated drawn fibres.

Characteristic of PA6-60 knitted fabrics

Figure 9 shows the images of untreated and treated PA6-60 knitted fabrics. Obvious differences between the untreated and treated fabrics can be seen from Figure 9. The untreated fabric with 40 wt% PP appears to be transparent under light microscope (Figure 9 b). The treated fabrics appears to be opaque and white in colour (Figure 9 b'). The removal of the PP from the knitted fabric results in a fabric with PA6 microfibres s as shown in Figure 9 (c').

The thickness of the untreated fabric, which has solid and round fibre structure, consist of PA6 microfibres encapsulate by the PP matrix, as shown in Figure 2 B-1. The removal of PP matrix collapses the fibre structure, releases the loose and flexible PA6 microfibres and directly reduce the fibre diameter which affect the fabric thickness. The elimination of approximately 40% of PP component also affect the fabric mass per unit area of the treated fabric. (Figure S10 and S11 for fabric thickness and mass per unit area, respectively were supplied in Supporting Information).

The structure of the fabric, however, was not significantly affected by the PP removal. The wales per inch of the fabric remains the same while the course per inch increases slightly after the treatment. The stitch density also increases slightly due to the shrinkage on course direction.

The ball burst strength results normalised to the fabric mass per unit area show that the treated fabrics has slightly improved ball burst strength than the untreated fabrics (see Figure S12 in Supporting Information). Other studies by Gun[34] and Srinivasan[35] also showed improvement in burst strength of fabrics from microfibres compared to the fabric from conventional fibres. The improved strength in microfibre fabrics can be attributed to the increased surfaced area and higher inter-fibre friction.[36,37]

Figure 10 shows the vertical wicking properties of the treated fabrics. As can be seen, the graphs in Figure 10 show no wicking properties of the untreated fabric as no wicking behaviour can be observed on the fabric. PA6-60 untreated fabrics produced from hybrid fibre of PP and PA6 with PP as a matrix thus, PP dominate the outer surface of the fabric. PP is a hydrophobic polymer thus hardly absorbs water. In addition, the fabric structure for this study was an open structure and therefore it resulted in creating big capillary gap between fibres. Treated fabric however shows good wicking behaviour with the course direction have greater wicking height. Treated fabrics contained PA6 microfibres with small capillary spaces between the microfibres. The capillary spaces improved the capillary pressure and enhance the wicking rate of the fabric.

Conclusions

The sorting of multi-material textile waste is challenging and processing of such waste into hybrid fibres can help to upcycle textile waste. In line with this, PA6:PP hybrid fibres were produced using single step twin-screw melt extrusion and processed in to PA6 microfibres by sacrificial removal of the PP component. The ratio and viscosity of component polymers affect the morphology of the fibre. PA6 was dispersed in the PP matrix in the PA6-50 and PA6-60 hybrid fibres while in the PA6-80, PA6 act as a matrix and encapsulate the PP. PA6-65 shows unique fibres morphology with PA6 dominantly surrounded the PP but also dispersed in the PP 'matrix' in small area of the fibres. The sacrificial removal of PP component in PA6-50 and PA6-60 resulted in PA6 microfibres with mean diameter value below 2 μm. In addition, knitted fabrics were produced from PA6-60 hybrid fibre to study the performance advantages offered by the PA6 microfibre fabric. The comparison showed that micro-fibrillar structure resulted in improved wicking properties and bursting strength than untreated fabric. The advantages of producing microfibres in a single step melt extrusion includes processing of multi-material waste as well as production of microfibres by employing conventional textile extrusion technologies. The work can be extended to other polymer waste mixtures.

Funding

This research did not receive any specific grant from funding agencies in the public, commercial, or non-for-profit sectors.

References

1. Roeder J, Oliveira RVB, Gonçalves MC, Soldi V, Pires ATN. Polypropylene/polyamide-6 blends: Influence of compatibilizing agent on interface domains. *Polym Test*. 2002;21(7):815-821. doi:10.1016/S0142-9418(02)00016-8
2. Ellen MacArthur Foundation. A New Textiles Economy: Redesigning Fashion's Future. https://www.ellenmacarthurfoundation.org/publications. Published 2017. Accessed August 20, 2018.
3. Jaziri M, Barhoumi N, Massardier V, Mélis F. Blending PP with PA6 industrial wastes: Effect of the composition and the compatibilization. *J Appl Polym Sci*. 2008;107:3451-3458. doi:10.1002/app
4. Asiaban S, Moradian S. Investigation of tensile properties and dyeing behavior of various polypropylene/amine modifier blends. *J Appl Polym Sci*. 2012;123:2162-2171.

doi:10.1002/app

5. Liao HY, Zheng LY, Hu YB, et al. Dynamic rheological behavior of reactively compatibilized polypropylene/polyamide 6 blending melts. *J Appl Polym Sci*. 2015;132(24):1-8. doi:10.1002/app.42091
6. Yoon BS, Joang JY, Suh MH, Lee YM, Lee SH. Mechanical properties of polypropylene/polyamide 6 blends: Effect of manufacturing processes and compatibilization. *Polym Compos*. 1997;18(6):757-764. doi:10.1002/pc.10328
7. Ďurčová O, Gróf I, Jambrich M, Mizerák P. Fibres from polypropylene/polyamide 6 blends: Application of FT-IR Dichroism for study of fibre molecular orientation. *Polym Test*. 1992;11(3):193-203. doi:10.1016/0142-9418(92)90050-L
8. Hajiraissi R, Jahani Y, Hallmann T. Investigation of rheology and morphology to follow physical fibrillar network evolution through fiber spinning of PP/PA6 Blend Fiber. *Polym Eng Sci*. 2017:1-10. doi:10.1002/pen
9. Liang B, White JL, Spruiell JE. Polypropylene/nylon 6 blends: Phase distribution morphology, rheological measurements and structure development in melt spinning. *J Appl Polym Sci*. 1983;28:2011-2032.
10. Takahashi T, Konda A, Shimizu Y. The changes of structure and tensile strength and elongation characteristics for the polypropylene/polyamide 6 blend fibers upon drawing. *Sen'i Gakkaishi*. 1996;52(8):38-46.
11. Afshari M, Kotek R, Kish MH, Dast HN, Gupta BS. Effect of blend ratio on bulk properties and matrix-fibril morphology of polypropylene / nylon 6 polyblend fibers. *Polymer (Guildf)*. 2001;43(2002):1331-1341.
12. Kunchimon SZ, Tausif M, Goswami P, Cheung V. Polyamide 6 and thermoplastic polyurethane recycled hybrid Fibres via twin-screw melt extrusion. *J Polym Res*. 2019;26(7). doi:10.1007/s10965-019-1827-0
13. Potente H, Bastian M, Gehring A, Stephan M, Pötschke P. Experimental investigation of the morphology development of polyblends in corotating twin-screw extruders. *J Appl Polym Sci*. 2000;76(5):708-721. doi:10.1002/(SICI)1097-4628(20000502)76:5<708::AID-APP13>3.0.CO;2-1
14. Takahashi T, Konda A, Shimizu Y. Effect of viscosity ratio on structure of polypropylene / polyamide 6 blend fiber. 1996;52(10):507-515.
15. Wang L, Guo Z-X, Yu J. Cocontinuous phase morphology for an asymmetric composition of polypropylene/polyamide 6 blend by melt mixing of polypropylene with premelted polyamide 6/organoclay masterbatch. *J Appl Polym Sci*. 2012;123:1218-1226. doi:10.1002/app.34600
16. Jordhamo GM, Manson JA, Sperling LH. Phase continuity and inversion in polymer blends and simultaneous interpenetrating networks. *Polym Eng Sci*. 1986;26(8):517-524. doi:10.1002/pen.760260802
17. Afshari M, Kotek R, Gupta BS, Kish MH, Dast HN. Mechanical and structural properties of melt spun polypropylene/nylon 6 alloy filaments. *J Appl Polym Sci*. 2005;97(2):532-544. doi:10.1002/app.21772
18. Sichina WJ. *DSC as Problem Solving Tool: Measurement of Percent Crystallinity of Thermoplastics*.; 2000. http://scholar.google.com/scholar?hl=en&btnG=Search&q=intitle:DSC+as+Problem+Solving+Tool+:+Measurement+of+Percent+Crystallinity+of+Thermoplastics#0.
19. Martin C. Twin screw extrusion for pharmaceutical processes. In: Repka M., Langley N,

DiNunzio J, eds. *Melt Extrusion; Materials, Technology and Drug Product Design*. Springer; 2013:47-79. doi:10.1007/978-1-4614-8432-5

20. Kirchhoff J. Mixing and Dispersing : Principles. In: Kohlgrüber K, ed. *Co-Rotating Twin-Screw Extruders: Fundamentals, Technology and Applications*. Carl Hanser Publisher; 2007:159-179.
21. Valles-Lluch A, Camacho W, Ribes-Greus A, Karlsson S. Influence of water on the viscoelastic behavior of recycled nylon 6,6. *J Appl Polym Sci*. 2002;85(10):2211-2218. doi:10.1002/app.10838
22. BASF. *Mechanical Performance of Polyamides with Influence of Moisture and Temperature–Accurate Evaluation and Better Understanding*.; 2003.
23. Zhang P, Xu D, Xiao R. Morphology development and size control of PA6 nanofibers from PA6/CAB polymer blends. *J Appl Polym Sci*. 2015;132(27):1-8. doi:10.1002/app.42184
24. Hasegawa T, Mikuni T. Higher-order structural analysis of nylon-66 nanofibers prepared by carbon dioxide laser supersonic drawing and exhibiting near-equilibrium melting temperature. *J Appl Polym Sci*. 2014;40361:n/a. doi:10.1002/app.40361
25. Koteswararao PR, Tulasi SL, Pavani Y. Impact of Solvents on Environmental Pollution. *J Chem Pharm Sci*. 2014;(3):132-135. doi:10.1016/0300-483X(94)90042-6
26. Berber E, Horzum N, Hazer B, Demir MM. Solution electrospinning of polypropylene-based fibers and their application in catalysis. *Fibers Polym*. 2016;17(5):760-768. doi:10.1007/s12221-016-6183-7
27. Goswami P, Blackburn RS, Taylor J, White P. Sorption of dyes on cellulose II: Effect of alkali treatment of fibre and dye structure. *Cellulose*. 2011;18(4):1063-1072. doi:10.1007/s10570-011-9540-0
28. Millot C, Fillot L., Lame O, Sotta P, Seguela R. Assessment of polyamide-6 crystallinity by DSC: Temperature dependence of the melting enthalpy. *J Therm Anal Calorim*. 2015;122(1):307-314. doi:10.1007/s10973-015-4670-5
29. Schick C. Differential scanning calorimetry (DSC) of semicrystalline polymers. *Anal Bioanal Chem*. 2009;395(6):1589-1611. doi:10.1007/s00216-009-3169-y
30. Jafari SH, Gupta AK. Crystallization behavior of polypropylene in polypropylene / nylon 6 blend. *J Appl Polym Sci*. 1998;71(May):1153-1161.
31. Jose S, Santhosh Aprem A, Thomas S, Francis B, Parameswaranpillai J. Thermal degradation and crystallization characteristics of multiphase polymer systems with and without compatibilizer. *AIMS Mater Sci*. 2016;3(3):1177-1198. doi:10.3934/matersci.2016.3.1177
32. Ayad E, Cayla A, Rault F, et al. Influence of rheological and thermal properties of polymers during melt spinning on bicomponent fiber morphology. *J Mater Eng Perform*. 2016;(Ref 9). doi:10.1007/s11665-016-2193-2
33. Meyabadi TF, Mohaddes Mojtahedi MR, Mousavi Shoushtari S a. Melt spinning of reused nylon 6: structure and physical properties of as-spun, drawn, and textured filaments. *J Text Inst*. 2010;101(6):527-537. doi:10.1080/00405000802561085
34. Gun AD. Dimensional, physical and thermal comfort properties of plain knitted fabrics made from modal viscose yarns having microfibers and conventional fibers. *Fibers Polym*. 2011;12(2):258-267. doi:10.1007/s12221-011-0258-2
35. Srinivasan J, Ramakrishnan G, Mukhopadhyay S, Manoharan S. A study of knitted fabrics from polyester microdenier fibres. *J Text Inst*. 2007;98(1):31-35. doi:10.1533/joti.2005.0180

36. Kalyanaraman AR. Coefficient of friction between yarns and contact surfaces. *Indian J Text Res*. 1988;13(1):1-6.
37. Mukhopadhyay S, Ramakrishnan G. Microfibres. *Text Prog*. 2008;40(1):1-86. doi:10.1080/00405160801942585

Table 1 Morphology of the hybrid fibres based on Jhordomo model and experimental result

Fibres	PA6*	PP*	η_{PA6}	η_{PP}	Jhordomo value	Jhordomo model	Experimental
PA6-80	0.80	0.20	1000	150	1.7	PP as matrix	PA6 as matrix
PA6-65	0.65	0.35			3.6	PP as matrix	Semi cocontinuous
PA6-60	0.60	0.40			4.4	PP as matrix	PP as matrix
PA6-50	0.50	0.50			6.6	PP as matrix	PP as matrix

*Volume fraction of polymer

Table 2: Thermal properties of as-spun untreated fibres

Fibre (untreated)	*2nd Heating*		*Cooling*		*Melting enthalpy*		*Crystallinity*	
	$T_{m\,PP}$ (°C)	$T_{m\,PA6}$ (°C)	$T_{c\,PP}$ (°C)	$T_{c\,PA6}$ (°C)	ΔH_{PP} (J g^{-1})	ΔH_{PA6} (J g^{-1})	X_{PP} (%)	X_{PA6} (%)
PA6	-	221	-	188	-	58.4	-	25.4
PA6-80	160	221	120	187	14.6	44.6	34.8	24.2
PA6-65	163	221	122	187	24.2	31.4	33.0	21.0
PA6-60	163	221	118	187	31.5	33.7	37.7	24.4
PA6-50	161	221	116	188	46.5	24.9	44.4	21.6
PP	160	-	113	-	102.8	-	49.1	-

Table 3: Thermal properties of as-spun treated fibres

Fibre (treated)	*Heating*		*Cooling*		*Melting enthalpy*		*Crystallinity*	
	$T_{m\,PP}$ (°C)	$T_{m\,PA6}$ (°C)	$T_{c\,PP}$ (°C)	$T_{c\,PA6}$ (°C)	ΔH_{PP} (J g^{-1})	ΔH_{PA6} (J g^{-1})	X_{PP} (%)	X_{PA6} (%)
PA6-80	160	221	120	187	13.5	41.3	32.3	22.4
PA6-65	163	220	122	186	20.8	34.5	28.4	23.1
PA6-60	-	221	121	186	-	49.0	-	21.3
PA6-50	-	222	-	187	-	55.2	-	24.0

Table 4 TGA result of as-spun hybrid fibres (untreated and treated)

Fibre	Untreated				Treated			
	T_{onset} (°C)	T_{50} (°C)	T_{max} (°C)	Residue (%)	T_{onset} (°C)	T_{50} (°C)	T_{max} (°C)	Residue (%)
PA6	413	445	455	2.2	-	-		-
PP-20	415	445	457	1.3	419	448	462	-3.6
PP-35	415	434	467	-1.0	409	446	462	1.6
PP-40	422	451	466	1.7	411	442	455	2.0
PP-50	419	448	463	1.1	407	442	449	5.9
PP	432	458	465	0.83	-	-		-

Figure legends

Figure 1 The morphology of PA6:PP blend categorised as Structure I and Structure II.

Figure 2 SEM micrograph of the PA6:PP fibres before treatment (*x*-1), after treated with toluene; as-spun fibre cross-section view (*x* -2), as-spun fibre longitudinal view (*x* -3) and drawn fibre longitudinal view (*x* -4).

Figure 3 Micrograph of pure and hybrid fibres taken using light microscope (Leica M205C).

Figure 4 Microfibres diameter of as-spun fibre and drawn for PA6-65, PA6-60 and PA6-50. (n=30)

Figure 5 DSC curves of as-spun (untreated and treated) fibre for second heating cycle.

Figure 6 Thermal degradation of the as-spun hybrid fibres (untreated); a) TGA curve and b) derivative weight

Figure 7 Tenacity of as-spun and drawn fibres (untreated and treated).

Figure 8 Tenacity vs breaking elongation of drawn untreated and treated hybrid fibres, PA6 and PP.

Figure 9 Structure of the PA6-60 knitted fabric; untreated fabrics (a-c) and treated fabrics after removal of the PP component (a'-c') at different magnification viewed under light microscope (a, b, a' & b') and SEM (c & c').

Figure 10 Wicking properties of treated fabric in wale and course direction.

Supporting Information (Figure legends)

Figure S1 The rheology of PA6 and PP at 230 °C.

Figure S2 Schematic diagram of two immiscible polymer blend fibre with different composition of polymer A to polymer B; a) polymer A as a major component, b) co-continuous phase when the composition of two polymers are almost the same, c) polymer A as a minor component.

Figure S3 Fibre diameter of as-spun fibre and drawn for PA6-65, PA6-60 and PA6-50. (n=30)

Figure S4 PA6 microfibres diameter distribution for as-spun and drawn fibres. (n=50)

Figure S5 DSC curves of as-spun (untreated and treated) fibres for cooling cycle.

Figure S6 Thermal degradation of the as-spun hybrid fibres after the treatment with toluene; a) TGA curve and b) derivative weight.

Figure S7 Breaking elongation for as-spun and drawn fibres (untreated and treated).

Figure S8 Tenacity vs breaking elongation of as-spun untreated and treated hybrid fibres, PA6 and PP.

Figure S9 Young's modulus of as-spun and drawn fibres (untreated and treated).

Figure S10 Mass per unit area and thickness of untreated and treated fabrics

Figure S11 Courses, wales and stitch density of untreated and treated fabrics

Figure S12 Ball burst strength of untreated and treated fabrics.

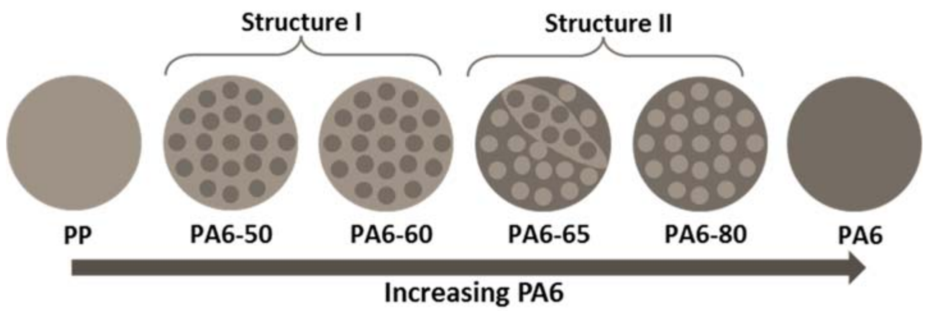

Figure 1 The morphology of PA6:PP blend categorised as Structure I and Structure II.

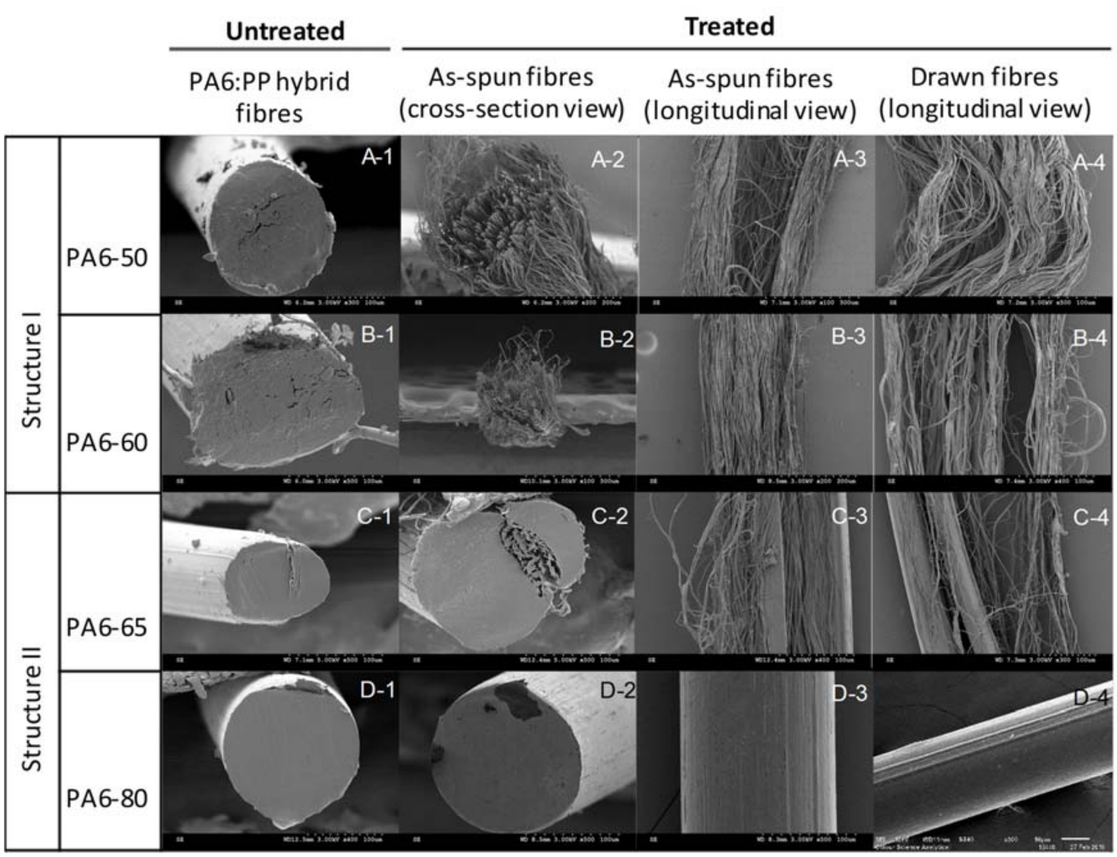

Figure 2 SEM micrograph of the PA6:PP fibres before treatment (*x*-1), after treated with toluene; as-spun fibre cross-section view (*x* -2), as-spun fibre longitudinal view (*x* -3) and drawn fibre longitudinal view (*x* -4).

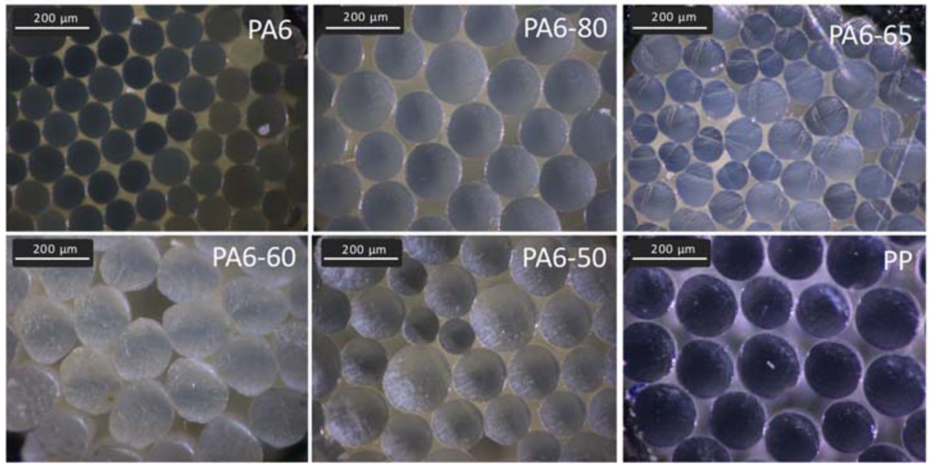

Figure 3 Micrograph of pure and hybrid fibres taken using light microscope (Leica M205C).

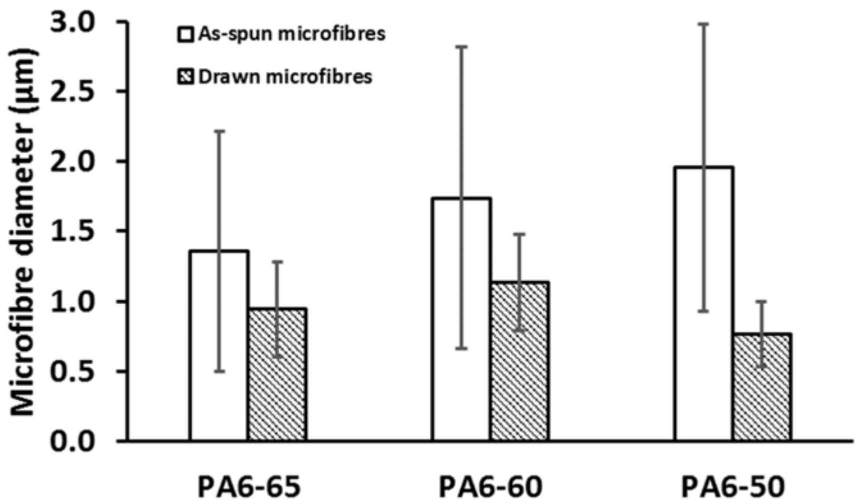

Figure 4 Microfibres diameter of as-spun fibre and drawn for PA6-65, PA6-60 and PA6-50. (n=30)

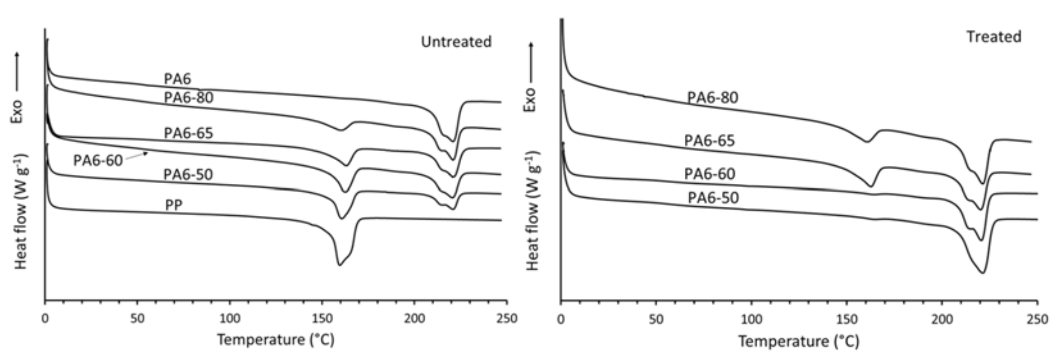

Figure 5 DSC curves of as-spun (untreated and treated) fibre for second heating cycle.

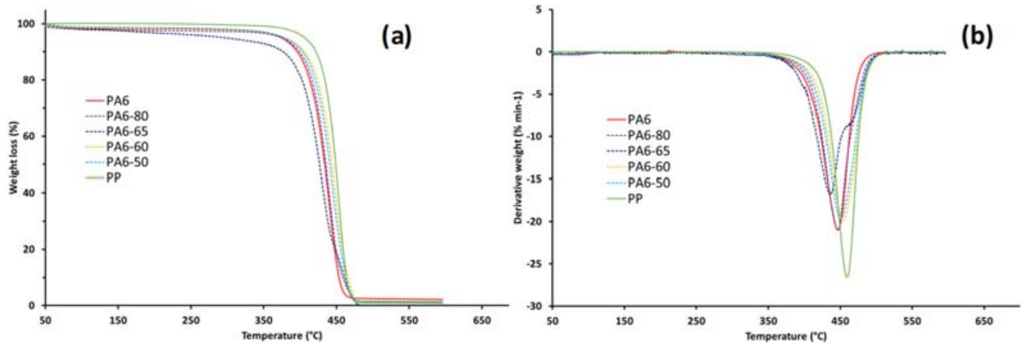

Figure 6 Thermal degradation of the as-spun hybrid fibres (untreated); a) TGA curve and b) derivative weight

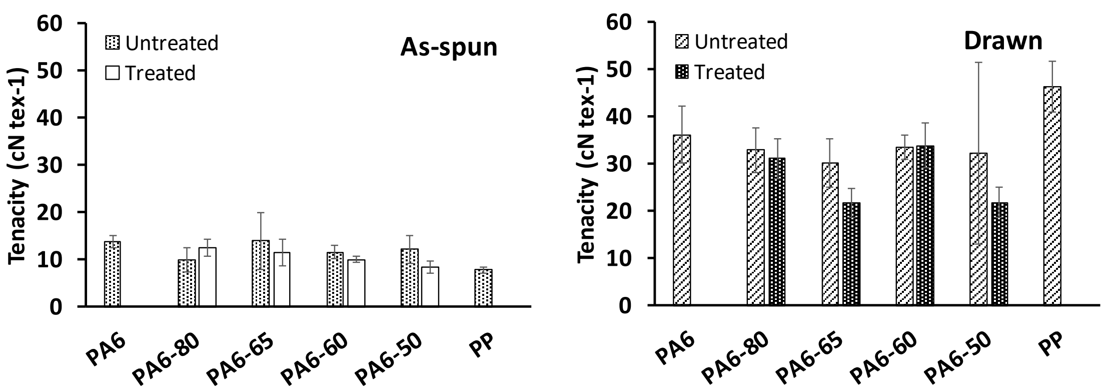

Figure 7 Tenacity of as-spun and drawn fibres (untreated and treated).

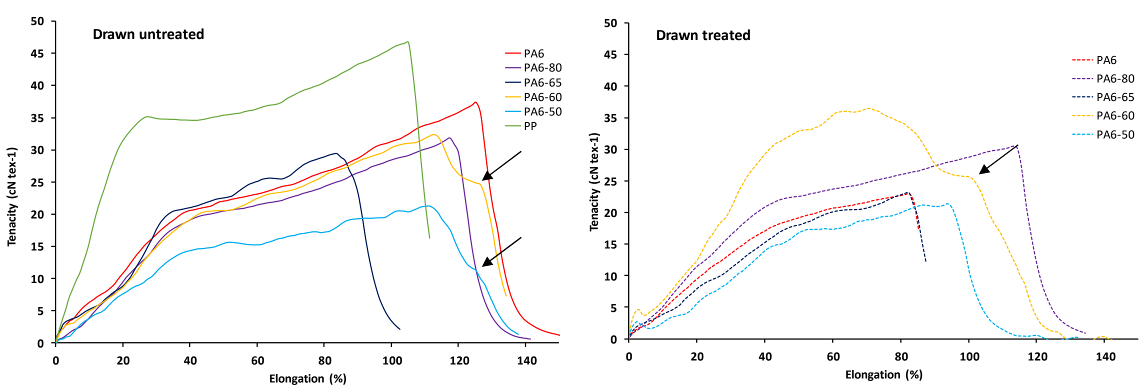

Figure 8 Tenacity vs breaking elongation of drawn untreated and treated hybrid fibres, PA6 and PP.

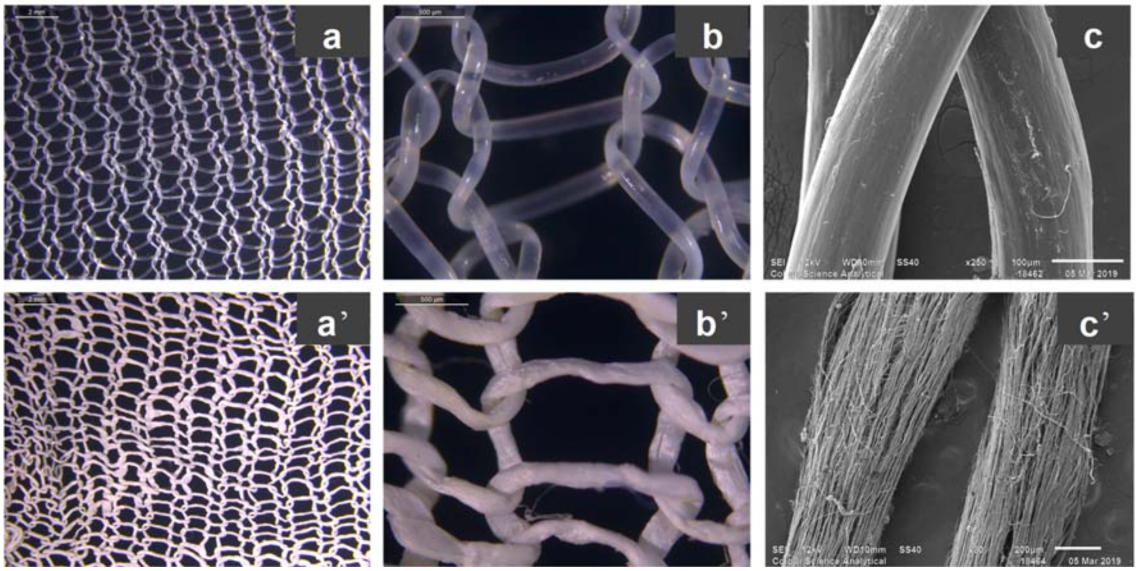

Figure 9 Structure of the PA6-60 knitted fabric; untreated fabrics (a-c) and treated fabrics after removal of the PP component (a'-c') at different magnification viewed under light microscope (a, b, a' & b') and SEM (c & c').

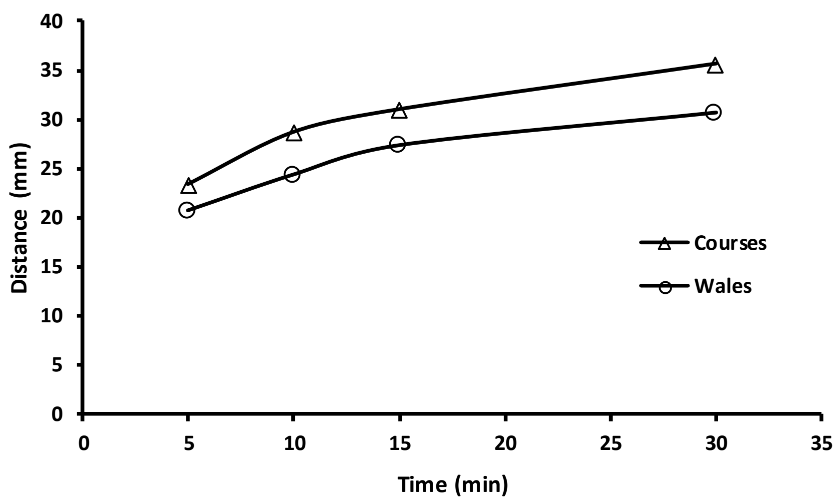

Figure 10 Wicking properties of treated fabric in wale and course direction.

Supporting Information

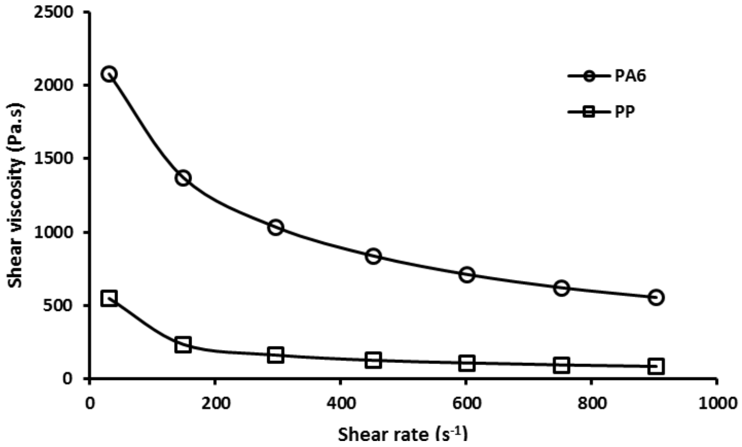

Figure S1 The rheology of PA6 and PP at 230 °C.

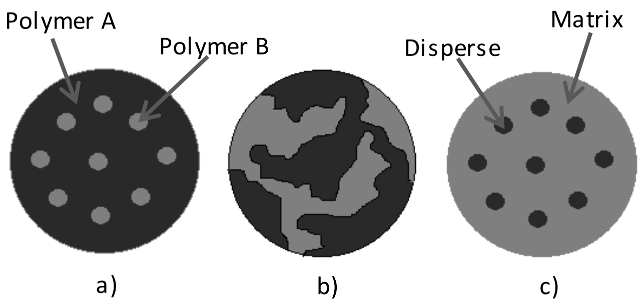

Figure S2 Schematic diagram of two immiscible polymer blend fibre with different composition of polymer A to polymer B; a) polymer A as a major component, b) co-continuous phase when the composition of two polymers are almost the same, c) polymer A as a minor component.

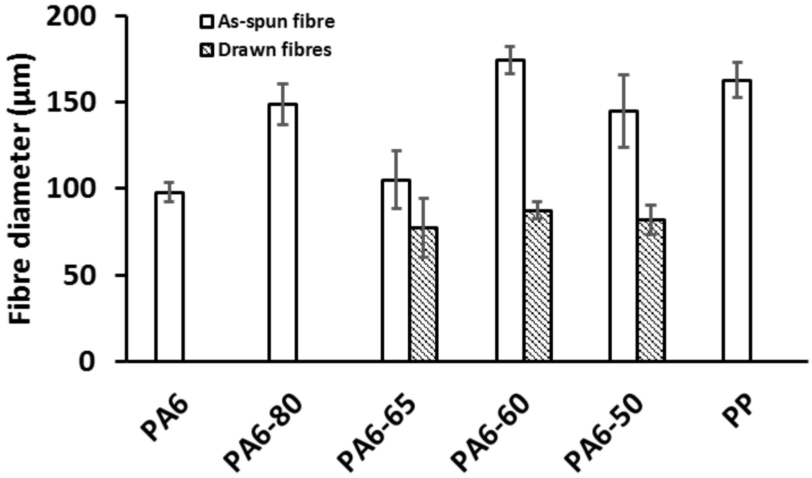

Figure S3 Fibre diameter of as-spun fibre and drawn for PA6-65, PA6-60 and PA6-50. (n=30)

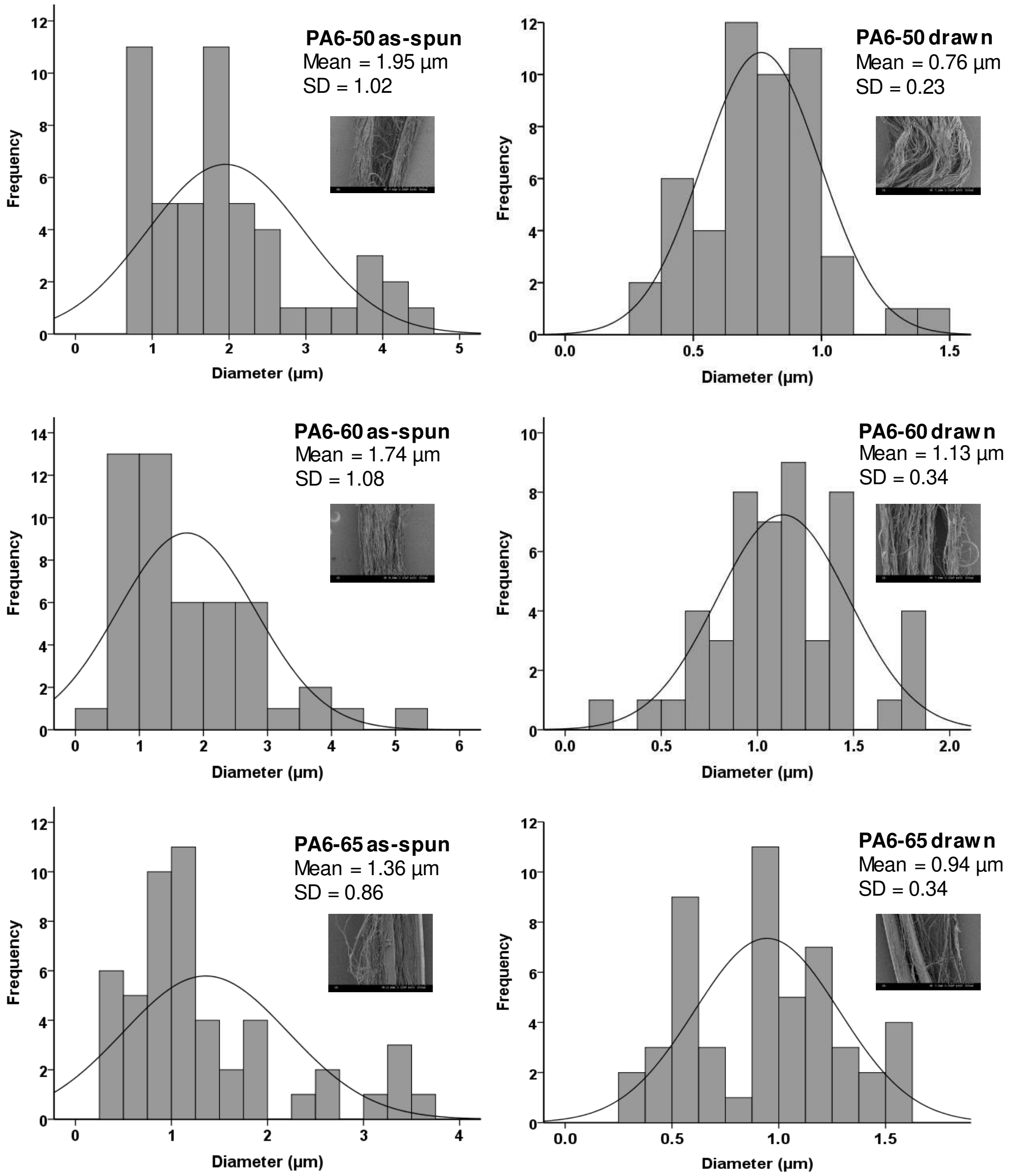

Figure S4 PA6 microfibres diameter distribution for as-spun and drawn fibres. (*n*=50)

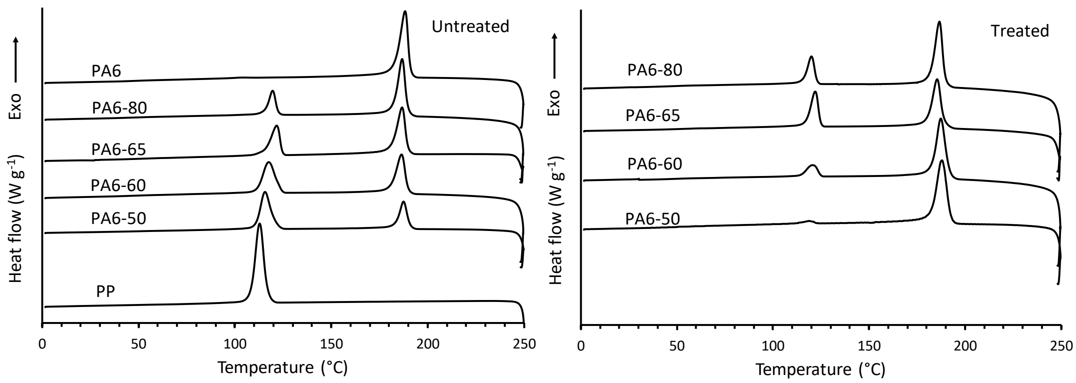

Figure S5 DSC curves of as-spun (untreated and treated) fibres for cooling cycle.

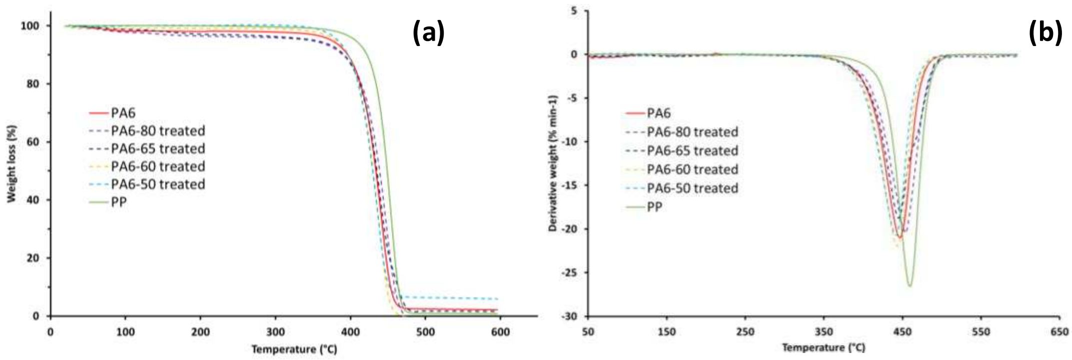

Figure S6 Thermal degradation of the as-spun hybrid fibres after the treatment with toluene; a) TGA curve and b) derivative weight

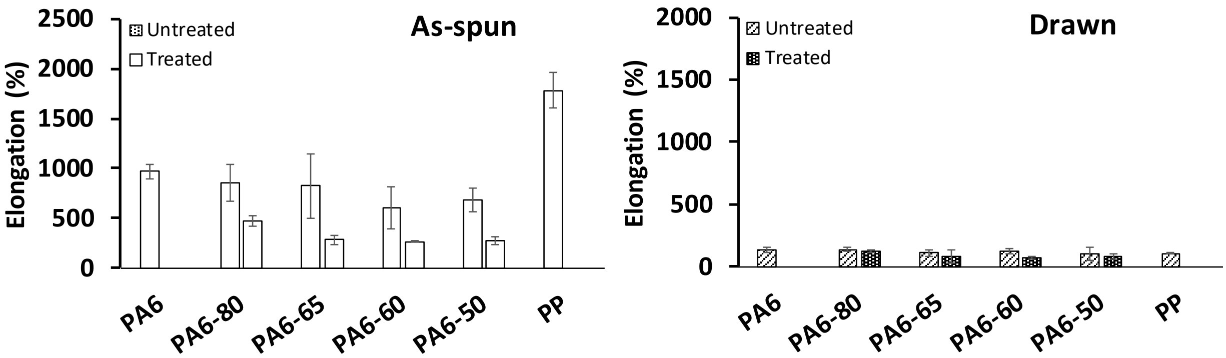

Figure S7 Breaking elongation for as-spun and drawn fibres (untreated and treated).

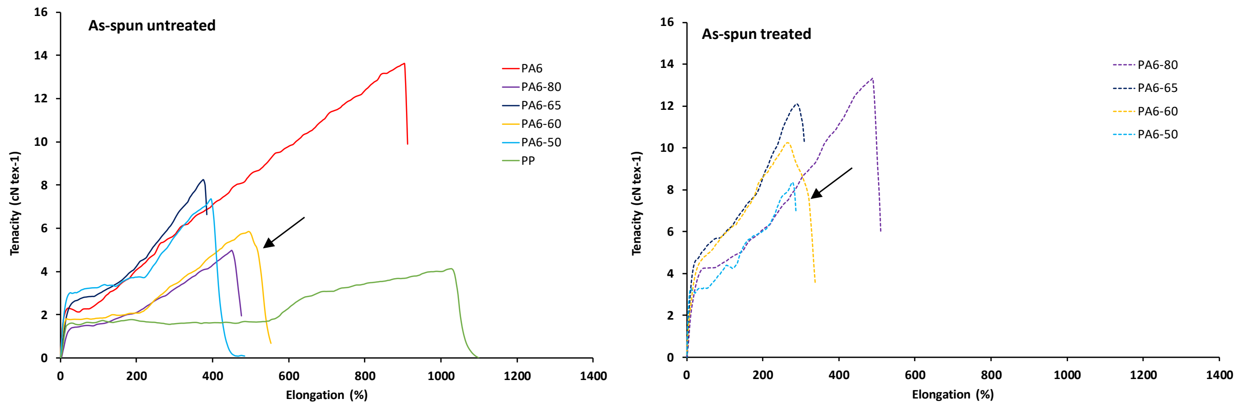

Figure S8 Tenacity vs breaking elongation of as-spun untreated and treated hybrid fibres, PA6 and PP.

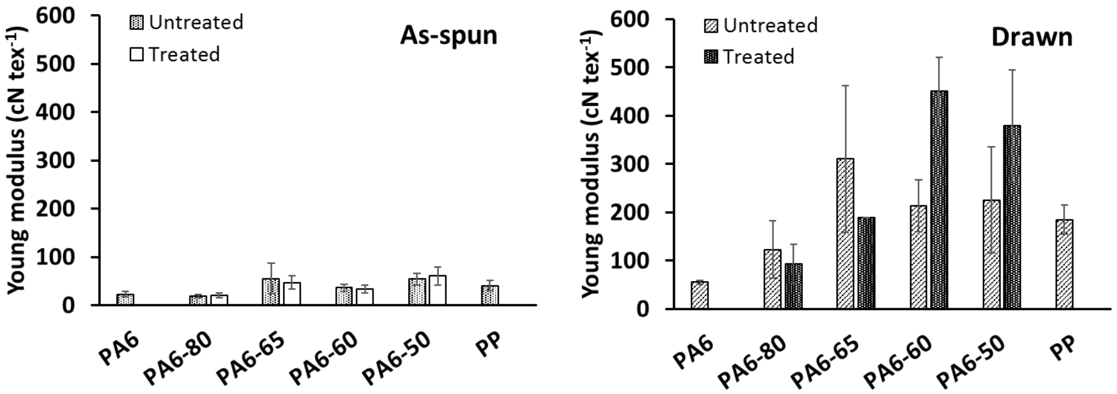

Figure S9 Young's modulus of as-spun and drawn fibres (untreated and treated).

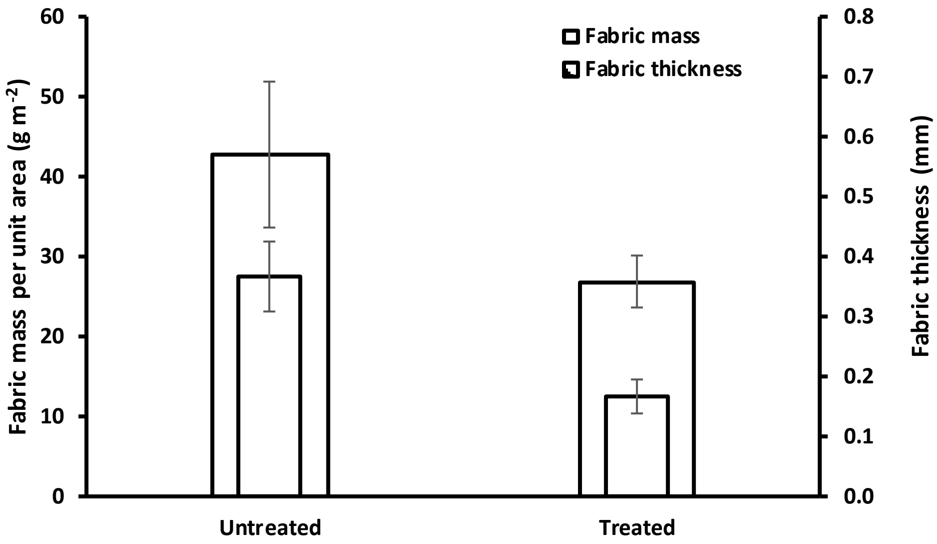

Figure S10 Mass per unit area and thickness of untreated and treated fabrics.

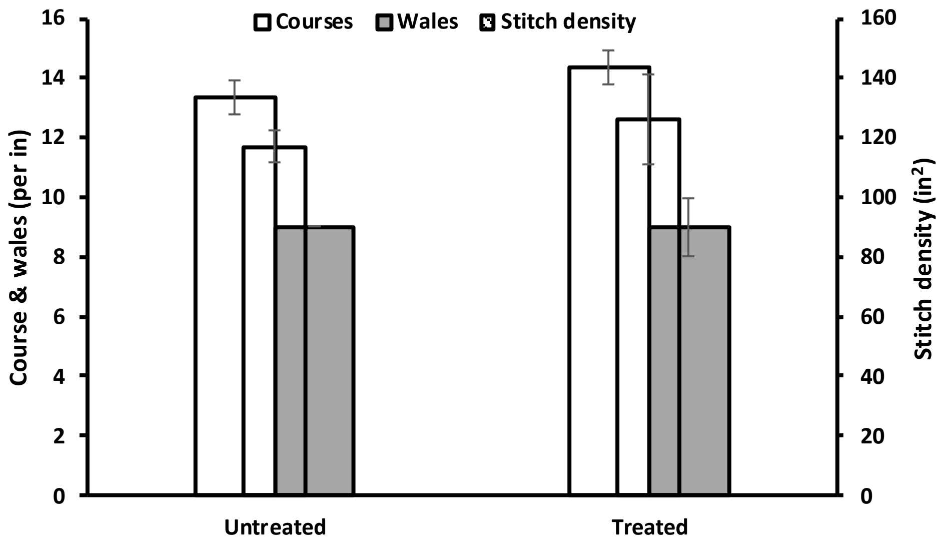

Figure S11 Courses, wales and stitch density of untreated and treated fabrics.

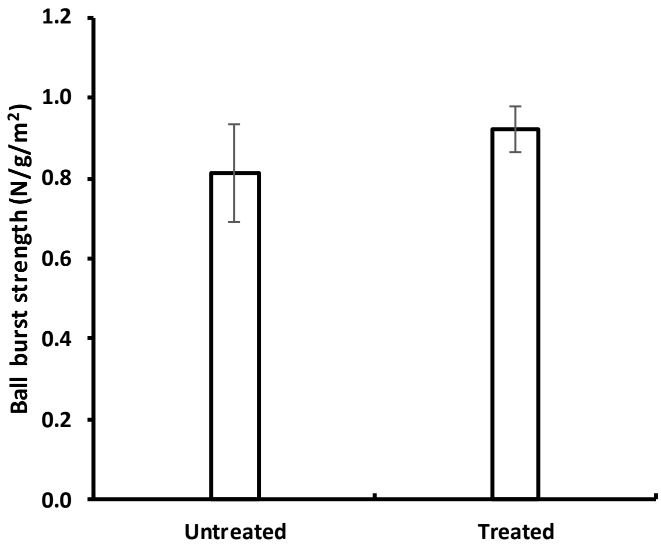

Figure S12 Ball burst strength of untreated and treated fabrics.